PHYSICAL REVIEW A **93**, 061601(R) (2016)

Synthetic-gauge-field stabilization of the chiral-spin-liquid phase

Gang Chen,[1,2,*] Kaden R. A. Hazzard,[3,4] Ana Maria Rey,[5,6] and Michael Hermele[7,6]
[1]*State Key Laboratory of Surface Physics, Center for Field Theory and Particle Physics, Department of Physics, Fudan University, Shanghai 200433, China*
[2]*Collaborative Innovation Center of Advanced Microstructures, Fudan University, Shanghai 200433, China*
[3]*Department of Physics and Astronomy, Rice University, Houston, Texas 77005, USA*
[4]*Rice Center for Quantum Materials, Rice University, Houston, Texas 77005, USA*
[5]*JILA and Department of Physics, University of Colorado–Boulder, NIST, Boulder, Colorado 80309-0440, USA*
[6]*Center for Theory of Quantum Matter, University of Colorado, Boulder, Colorado 80309, USA*
[7]*Department of Physics, University of Colorado–Boulder, Boulder, Colorado 80309-0440, USA*
(Received 13 February 2015; revised manuscript received 30 July 2015; published 9 June 2016)

We explore the phase diagram of the SU(N) Hubbard models describing fermionic alkaline-earth-metal atoms in a square optical lattice with, on average, one atom per site, using a slave rotor mean-field approach. We find that the chiral spin liquid (CSL) predicted for $N \geqslant 5$ and large interactions passes through a fractionalized state with a spinon Fermi surface as interactions are decreased before transitioning to a weakly interacting metal. We show that by adding a uniform artificial gauge field with $2\pi/N$ flux per plaquette, the CSL becomes the ground state for all $N \geqslant 3$ at intermediate interactions, persists to weaker interactions, and exhibits a larger spin gap. For $N \geqslant 5$ we find the CSL is the ground state everywhere the system is a Mott insulator. The gauge field stabilization of the CSL at lower interactions, and thus at weaker lattice depths, together with the increased spin gap, can relax the temperature constraints required for its experimental realization in ultracold atom systems.

DOI: 10.1103/PhysRevA.93.061601

Introduction. Topologically ordered phases [1] are of fundamental interest, as they exist outside of the Landau symmetry-breaking paradigm for classifying phases of matter and display exotic phenomena such as fractionalized excitations [2]; in some cases these phases may be useful for topological quantum computation [3,4]. The experimental realization of topological order beyond the fractional quantum Hall effects is a major goal in modern condensed matter. Ultracold atomic systems, with their unique tunability and control, may offer a promising platform to realize topological and exotic phases.

It was recently proposed [5–7] and experimentally confirmed [8–13] that fermionic alkaline-earth-metal atoms (AEA) exhibit SU(N) symmetric interactions. The value of N can be controllably varied by initial-state preparation up to $2I+1$, with I being the nuclear spin (as large as $N=10$ for ^{87}Sr with $I=9/2$). Recently ultracold atom experiments have trapped and cooled AEA to quantum degeneracy and loaded them in an optical lattice [14–24]. Evidence of cooling effects arising from the large spin entropy have also been reported [12,25,26]. In fact, experiments are beginning to reach the regime where short-range spin correlations develop and thus it is particularly timely to study quantum magnetism in these systems.

Most of the current theoretical work has focused on the strongly interacting limit where the SU(N) Hubbard model reduces to a SU(N) Heisenberg model. In fact, spin models exhibiting SU(N) symmetry have stimulated various theoretical investigations that predict exotic ground states [26–44], some of them featuring topological order such as the long-sought chiral spin liquid (CSL) [28,34]. These phases are stabilized because the large Hilbert space of a SU(N) local moment allows the spins to fluctuate more efficiently, delocalizing the spins and suppressing magnetic order in a similar way to that of geometric frustration. However, reaching the strongly interacting regime is experimentally challenging and imposes strong temperature constraints, since it is achieved at very deep lattices where tunneling is exponentially suppressed and energy scales become extremely low. It is then highly desirable to determine under what conditions the CSL can be stabilized at lower lattice depths (i.e., weaker interaction strengths).

In this Rapid Communication we study the SU(N) Hubbard models on a square optical lattice at an average filling lattice of one atom per site and show that the CSL phase extends to intermediate interacting regimes. We also find that at weaker interactions another exotic phase, namely the gapless quantum spin liquid with a spinon Fermi surface [45,46], emerges. Moreover, we predict that the presence of a a synthetic gauge field [47–54], generated for example by light-induced hopping [55–57], enhances the parameter space of the CSL, pushes its existence to lower interactions and increases the corresponding spin gap. Operating at weaker lattice depths, where the absolute energy scales are more favorable, can relax the temperature constrains required for the emergence of topological or magnetic order. We expect consequently that the conclusions presented in this work are useful for the implementation of new states of matter in cold atomic systems.

AEA in optical lattices with synthetic gauge fields. AEA in a sufficiently deep optical lattice are described by a SU(N) generalization of the usual ($N=2$) Hubbard model,

$$H = -t \sum_{\langle i,j\rangle,\alpha} e^{i\phi_{ij}} c^{\dagger}_{\alpha,i} c_{\alpha,j} + \frac{U}{2} \sum_{i} (n_i - 1)^2, \qquad (1)$$

*chggst@gmail.com

where $c_{\alpha,i}$ is the fermionic annihilation operator for nuclear spin state α at lattice site i, $\sum_{\langle i,j\rangle}$ indicates a sum over nearest neighbors i and j, and $\phi_{ij} = -\phi_{ji}$ is the (externally imposed) lattice gauge field. We define $n_i = \sum_\alpha c^\dagger_{\alpha,i} c_{\alpha,i}$, and t and U are the hopping energy and on-site interaction energy, whose ratio can be tuned by modifying the optical lattice depth. In this Rapid Communication, we take the average fermion number per site to be one.

The gauge field ϕ_{ij} depends both on the artificial electromagnetic field as well as the gauge choice. We are interested in the physics of a two-dimensional square lattice with a spatially uniform, time-independent artificial magnetic field, and use the Landau gauge where

$$\phi_{ij} = \begin{cases} \Phi x_j \delta_{y_j-1,y_i} & \text{if } \{i,j\} \text{ bond is vertical} \\ 0 & \text{otherwise,} \end{cases} \tag{2}$$

x_j is the x coordinate of site j measured in lattice units, and Φ is the flux penetrating a single square plaquette of the lattice [58]. We focus on the case $\Phi = 2\pi/N$, because this choice of Φ is favorable for the existence of the chiral spin liquid. We note that the magnetic unit cell associated with the translational invariance of the Hamiltonian is enlarged from the one imposed by the optical lattice potential. Figure 1(d) shows the system with this flux and gauge choice, and the enlarged magnetic unit cell, for $N = 3$.

The phase diagram and properties of this system are calculated within a slave rotor mean-field approximation [46,59], which we describe briefly. This technique is designed to match the previous large-N solution in the large U/t limit, and is well suited for describing nonmagnetic ground states in proximity to the Mott transition. First we expand the Hilbert space to include a U(1) bosonic rotor degree of freedom on each site, θ_j, and new fermionic spinon degrees of freedom associated with operators $f_{\alpha,j}$, which are defined by

$$c_{\alpha,j} = e^{-i\theta_j} f_{\alpha,j}. \tag{3}$$

To recover the original Hilbert space, we must impose the constraint

$$L_j = \sum_\alpha f^\dagger_{\alpha,j} f_{\alpha,j} - 1 \tag{4}$$

that the rotor angular momentum L_j is uniquely determined by the particle number. Here, L_j satisfies $[\theta_j, L_j] = i$. We rewrite the Hamiltonian in terms of these variables, giving

$$H = -t \sum_{\langle i,j\rangle,\alpha} e^{i\phi_{ij}} e^{i(\theta_i-\theta_j)} f^\dagger_{\alpha,i} f_{\alpha,j} + \frac{U}{2} \sum_i L_i^2. \tag{5}$$

Although the rewritten Hamiltonian Eq. (5), together with the constraint Eq. (4), is exactly equivalent to Eq. (1), to make further progress we make a mean-field approximation to decouple the rotor and spinon degrees of freedom. We then obtain the coupled mean-field Hamiltonians for the rotors and the spinons,

$$H_r = -\sum_{\langle i,j\rangle} J_{ij} e^{i\theta_i - i\theta_j} + \sum_i \frac{U}{2} L_i^2 + h_i(L_i + 1), \tag{6}$$

$$H_f = -\sum_{\langle i,j\rangle,\alpha} \tilde{t}_{ij} e^{i\phi_{ij}} f^\dagger_{\alpha,i} f_{\alpha,j} - \sum_{i,\alpha} h_i f^\dagger_{\alpha,i} f_{\alpha,i}, \tag{7}$$

where h_i is a Lagrange multiplier that enforces on average the constraint Eq. (4), $\tilde{t}_{ij} \equiv t\langle e^{i\theta_i - i\theta_j}\rangle_r$, and $J_{ij} \equiv t e^{i\phi_{ij}} \sum_\alpha \langle f^\dagger_{\alpha,i} f_{\alpha,j}\rangle_f$. Here the subindex r (f) refers to taking

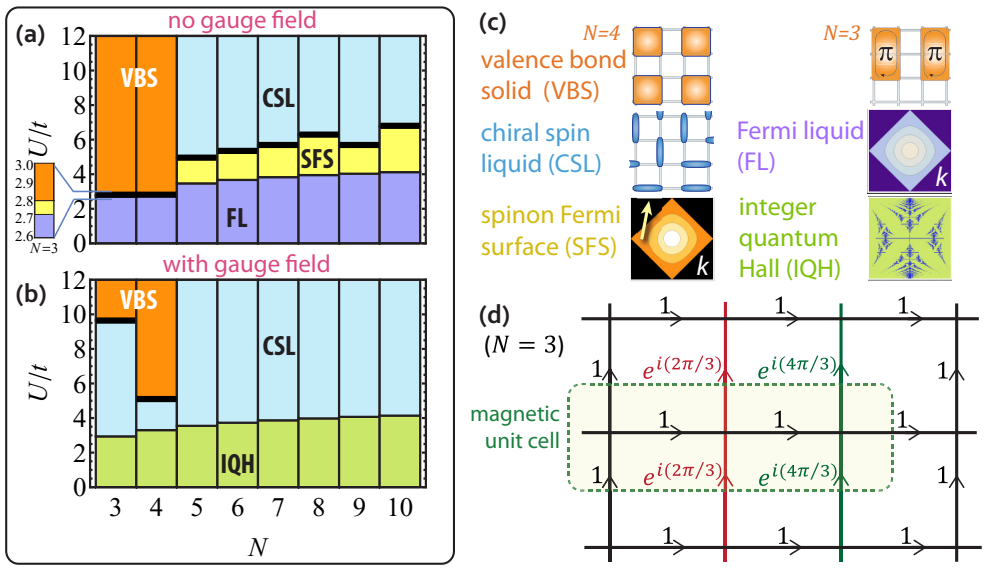

FIG. 1. Phase diagram, calculated with a slave-rotor mean-field approximation, as a function of spin flavor N and interaction strength U/t in the (a) absence and (b) presence of an artificial uniform magnetic field with flux per plaquette $\Phi = 2\pi/N$, illustrated in panel (d) for $N = 3$. Thin (thick) black lines are second-order (first-order) phase transitions. The states found are the valence bond solids (VBS), chiral spin liquid (CSL), spinon Fermi surface (SFS), Fermi liquid (FL), and integer quantum Hall (IQH) states. These are described in the text and illustrated in panel (c).

TABLE I. Parameters that characterize the obtained phases. The upper five (lower four) rows describe phases in the absence (presence) of the synthetic gauge field. The rotor (spinon) flux refers to the flux that is experienced by the rotor (spinon) in the mean-field Hamiltonian H_r (H_f). For the FL, SFS, IQH, and CSL states, the flux is defined for the elementary square plaquette. For SU(3)-VBS [SU(4)-VBS] state, the flux is defined through the 6-site [4-site] cluster [60].

Phases	$\langle e^{i\theta}\rangle$	Rotor flux	Spinon gap	Spinon flux
FL	$\neq 0$	0	0	0
SFS	0	0	0	0
CSL	0	$-2\pi/N$	$\neq 0$	$2\pi/N$
SU(3)-VBS	0	$-\pi$	$\neq 0$	π
SU(4)-VBS	0	0	$\neq 0$	0
IQH	$\neq 0$	0	$\neq 0$	$2\pi/N$
CSL	0	0	$\neq 0$	$2\pi/N$
SU(3)-VBS	0	$\pi/3$	$\neq 0$	π
SU(4)-VBS	0	$\pi/2$	$\neq 0$	0

the expectation value in the rotor (spinon) mean-field ground state $|\psi\rangle_r$ ($|\psi\rangle_f$). The Hamiltonians H_r and H_f are invariant under a U(1) gauge transformation, $f^\dagger_{\alpha,i} \to f^\dagger_{\alpha,i} e^{-i\chi_i}, \theta_i \to \theta_i + \chi_i$, and $\tilde{t}_{ij} \to \tilde{t}_{ij} e^{i\chi_i - i\chi_j}, J_{ij} \to J_{ij} e^{-i\chi_i + i\chi_j}$. We solve H_r and H_f self-consistently for several variational ansatz [60] and find the ground state by optimizing the total energy $\langle\psi|H|\psi\rangle$ where H is given by Eq. (5) and $|\psi\rangle \equiv |\psi\rangle_r|\psi\rangle_f$ is the mean-field state.

Phase diagrams. The slave-rotor mean-field phase diagram is displayed in Figs. 1(a) and 1(b). We find five phases: Fermi liquid (FL), integer quantum Hall (IQH), valence bond solids (VBS), a gapless spin liquid with a spinon Fermi surface (SFS) [45,46], and a CSL [61,62]. The noninteracting and the strong coupling (Heisenberg) limits are readily understood [28], and our slave-rotor mean-field results are compatible with the previous understanding. The VBS, SFS, and CSL are Mott insulating with uncondensed bosonic rotors $\langle e^{i\theta}\rangle = 0$. As we show in Table I, the rotor and the spinon may experience different, even opposite, gauge fluxes in their mean-field Hamiltonians for different phases. Since the rotor and the spinon must form a whole atom, the total gauge flux experienced by the rotor and the spinon should be equal to the synthetic gauge flux that is externally imposed on the atom.

We now describe the five different phases. The FL phase is very similar to the usual Fermi liquid except with N flavors of fermions [6]. The VBS are translation-symmetry-breaking phases with repeating units of SU(N) singlets spread across multiple sites. In particular, as we plot in Fig. 1(c), the system is decoupled into 6-site rectangular (4-site square) clusters in the SU(3)-VBS [SU(4)-VBS] state. The SFS spin liquid is characterized by a gapless spinon Fermi surface with a gapped bosonic rotor at the mean-field level. Going beyond the mean-field description, one needs to include the U(1) phase fluctuation of the spinon hopping $\tilde{t}_{ij}$. This is the internal gauge fluctuation [46]; it is dynamically generated and is unrelated to the synthetic gauge field that is imposed externally. At low energies, the SFS spin liquid is described by the spinon Fermi surface coupled to a fluctuating internal U(1) gauge field [46,63–67]. Due to the spinon-gauge coupling, the overdamped U(1) gauge boson scatters the spinons on the Fermi surface and destroys the coherence of the spinon quasiparticles. The resulting state is a non-Fermi liquid of fermionic spinons. In contrast, the spinons in the CSL form an integer quantum Hall state. Upon coupling to U(1) gauge fluctuations, this leads to a chiral topological order with anyon excitations and gapless chiral edge states carrying spin but no charge [61].

To understand the global structure of the phase diagram, it is useful to consider the $U/t = 0$ and $U/t \to \infty$ limits. The FL and IQH states are simply the noninteracting ground states at $U/t = 0$. In the strong coupling regime, the Hubbard model reduces to an SU(N) Heisenberg model, and the phase diagram coincides with previous slave-fermion mean-field results of the Heisenberg model [28]: For $N = 3,4$ the ground state is a VBS, while for $N \geqslant 5$ the ground state is a CSL. This is true both with and without a synthetic gauge field, as in the $U/t \to \infty$ limit the physics is governed by nearest neighbor superexchange, which is insensitive to the gauge flux. We note that numerical works on the SU(N) Heisenberg model found a 3-sublattice magnetic order for $N = 3$ [29] and a colored VBS order for $N = 4$ [31]. The discrepancy is probably because the slave-rotor decomposition does not provide a good description in the strong coupling regime for $N = 3,4$ [60].

In the intermediate U/t regime, the gauge field causes significant differences. Without a gauge field, we find that a SFS phase intervenes between the noninteracting FL and Heisenberg limit CSL or VBS for all N except $N = 4$, in which case there is a direct transition between the FL and VBS ground states. In contrast, the $\Phi = 2\pi/N$ gauge flux broadens the parameter space for which the CSL occurs: In addition to persisting down to $N = 3,4$, the CSL occurs immediately as the system becomes Mott insulating. A simple understanding of this comes from noting that the spinons occupy Landau levels if the spinons feel the same gauge field as the atoms. For $\Phi = 2\pi/N$ the spinons are at the proper filling to organize into an IQH state, which yields the CSL.

Now we discuss the phase transitions in the phase diagram. The nature of phase transitions is determined by examining the mean-field parameters. When the mean-field parameters vary continuously (abruptly) across the transition, the transition is continuous (first order). The SFS-CSL and FL-VBS transitions are first order, involving the breaking of time-reversal symmetry and lattice translation, respectively. The Mott transition, from FL to SFS (from IQH to CSL) in the absence (presence) of a gauge flux, is continuous and is expected to remain continuous beyond mean-field theory [68–70]. Because the SFS and the CSL are exotic phases with fractionalized excitations, the continuous Mott transitions are *not* described by any local order parameter and are beyond the Landau paradigm of symmetry-breaking phase transitions [68–70].

In the CSL, both the spinon sector and the rotor sector are gapped. Figure 2 illustrates the excitation gap Δ's dependence on U/t, N, and the gauge flux in the CSL where Δ is the smaller of the spin gap and the rotor gap. In the mean-field

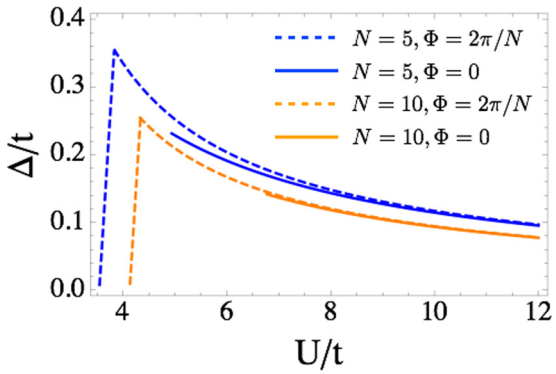

FIG. 2. The excitation gap of the CSL phase, Δ, as a function of interaction strength, U, both in units of the tunneling t. The curves illustrate the N and magnetic flux Φ dependence. From bottom to top, we show $(N = 10, \Phi = 0)$; $(N = 10, \Phi = 2\pi/10)$; $(N = 5, \Phi = 2\pi/5)$; and $(N = 5, \Phi = 2\pi/5)$. The cusps at $U/t \approx 4$ are the locations below which the rotor gap becomes smaller than the spin gap.

approximation, the spin gap is simply the band gap of the spinon spectrum, and the rotor gap is set by the Hubbard U interaction and thus stays much larger than the spin gap in the Mott insulating regime except near the Mott transition. For a given U/t, the spin gap slightly increases when the gauge field is turned on. An even more favorable effect of the gauge field for the spin gap occurs because the CSL persists to lower U/t. Since Δ increases as U/t decreases, the gauge field increases the maximum Δ by about a factor of 1.5. Note that Δ is normalized by t. Since t exponentially decreases with lattice depth even a factor of 1.5 enhancement of the gap in the intermediate lattice regime, in absolute energy units it corresponds to a significant enhancement compared to the same factor in the deep lattice limit. Moreover, because Δ sets the temperature to which the CSL's characteristics remain, we expect the gauge field to increase the temperature range over which the CSL behavior is accessible.

Gauge field implementation. One possibility is to use a Raman-induced tunneling scheme in the presence of a uniform potential gradient [52,53]. This scheme utilizes the optical lattice and generates the Hamiltonian Eq. (1) with strong gauge fluxes. An alternative scheme, natural for the present work with AEA, is the one that traps the $^1S_0$ ground (g) and $^3P_0$ excited (e) states in, for example, a checkerboard pattern in an optical lattice by using an appropriate, antimagic wavelength. This implementation generates a staggered flux and thus needs additional rectification to make it homogeneous [71]. For the latter we emphasize some points to consider in the presence of interactions: First, two e-state atoms on the same site can inelastically collide and be lost from the trap. We have found that this problem can be largely mitigated when using a checkerboard $g-e$ pattern [72]. Second, the interactions are inhomogeneous, being different for the sites occupied by g atoms and e atoms and could modify the discussed phase diagram.

Preparation and detection. Reaching the temperature regimes to observe the phase diagram (Fig. 1) is challenging. However, the expected advantage of the SU(N) symmetry for cooling [12,25,26,35] together with the less stringent temperature requirements to observe CSL phases in the presence of the synthetic gauge field might help achieve the required conditions. Other potentially favorable aspects of the gauge field are the absence of an intermediate SFS phase and that all transitions are second order in the mean-field analysis. Consequently, adiabatically going from weak to strong interactions may be easier than in the absence of the gauge field. On the other hand, the gauge field itself introduces further complications such as a complex band structure even in the weakly interacting regime. Consequently, determining optimal preparation is beyond the scope of this work. However, we point out that even if cooling temperature below the CSL gap is outside the current experimental reach, it is possible that certain features associated with the CSL may still be visible experimentally.

We briefly outline methods to detect the CSL and SFS. at a higher temperature. For example, the presence of time-reversal symmetry-breaking transition at a finite temperature as a consequence of the CSL phase at low temperatures should be observable in experiments without the synthetic gauge field. To detect the CSL, Ref. [34] suggests methods to probe two characteristic properties of topological phases: looking for topologically protected, chiral edge currents and introducing a weak attractive optical potential that is localized to a few lattice sites, which should bind the anyonic quasiparticles. Braiding or interfering these quasiparticles can manifest their anyonic nature. To detect the SFS state, one can perform spin-dependent Bragg spectroscopy to detect the 2-spinon continuum in the dynamic spin structure factor; the most basic signature of the exotic nature of this phase is the lack of order and existence of gapless excitations. More details of the state and its excitations could be revealed by considering more structure of the spectrum, similar to that considered in Refs. [73,74].

To summarize, we demonstrate that the SU(N) Hubbard model for $N \geqslant 3$ with or without a synthetic gauge flux on square optical lattice produces a rich phase diagram involving both non-Landau phases (like CSL and SFS phases) and non-Landau phase transitions. It is drastically different from the SU(2) Hubbard models with similar settings where a direct phase transition is found between a FL (a Dirac semimetal) for zero (π) gauge flux to a Neel state [75,76]. This further highlights the novel features brought by the SU(N) symmetry and the synthetic gauge flux.

Acknowledgments. This work was supported by the AFOSR, AFOSR-MURI, NSF JILA-PFC-1125844, NSF-PIF-1211914, NIST, and ARO (A.M.R.); the U.S. Department of Energy, Office of Science, Basic Energy Sciences, under Award No. DE-FG02-10ER46686 (G.C. and M.H.); and Simons Foundation Grant No. 305008 (M.H. sabbatical support). G.C. acknowledges NSF Grant No. PHY11-25915 for supporting the visitor program at the Kavli Institute for Theoretical Physics during the workshop "Frustrated Magnetism and Quantum Spin Liquids" in 2012, when and where part of the current work was done.

[1] Here we mean intrinsic topological order in the sense of gapped states with long-range quantum entanglements, which excludes, for example, topological band insulators.
[2] X. Wen, *Quantum Field Theory of Many-Body Systems: From the Origin of Sound to an Origin of Light and Electrons* (Oxford University Press, Oxford, 2007).
[3] A. Y. Kitaev, Ann. Phys. **303**, 2 (2003).
[4] C. Nayak, S. H. Simon, A. Stern, M. Freedman, and S. D. Sarma, Rev. Mod. Phys. **80**, 1083 (2008).
[5] C. Wu, J.-P. Hu, and S.-C. Zhang, Phys. Rev. Lett. **91**, 186402 (2003).
[6] M. A. Cazalilla, A. F. Ho, and M. Ueda, New J. Phys. **11**, 103033 (2009).
[7] A. V. Gorshkov, M. Hermele, V. Gurarie, C. Xu, P. S. Julienne, J. Ye, P. Zoller, E. Demler, M. D. Lukin, and A. M. Rey, Nat. Phys. **6**, 289 (2010).
[8] S. Stellmer, R. Grimm, and F. Schreck, Phys. Rev. A **84**, 043611 (2011).
[9] G. Pagano, M. Mancini, G. Cappellini, P. Lombardi, F. Schäfer, H. Hu, X.-J. Liu, J. Catani, C. Sias, M. Inguscio, and L. Fallani, Nat. Phys. **10**, 198 (2014).
[10] F. Scazza, C. Hofrichter, M. Höfer, P. C. D. Groot, I. Bloch, and S. Fölling, Nat. Phys. **10**, 779 (2014).
[11] G. Cappellini, M. Mancini, G. Pagano, P. Lombardi, L. Livi, M. Siciliani de Cumis, P. Cancio, M. Pizzocaro, D. Calonico, F. Levi, C. Sias, J. Catani, M. Inguscio, and L. Fallani, Phys. Rev. Lett. **113**, 120402 (2014).
[12] S. Taie, R. Yamazaki, S. Sugawa, and Y. Takahashi, Nat. Phys. **8**, 825 (2012).
[13] X. Zhang, M. Bishof, S. L. Bromley, C. V. Kraus, M. S. Safronova, P. Zoller, A. M. Rey, and J. Ye, Science **345**, 1467 (2014).
[14] Y. Takasu, K. Maki, K. Komori, T. Takano, K. Honda, M. Kumakura, T. Yabuzaki, and Y. Takahashi, Phys. Rev. Lett. **91**, 040404 (2003).
[15] T. Fukuhara, S. Sugawa, and Y. Takahashi, Phys. Rev. A **76**, 051604 (2007).
[16] S. Kraft, F. Vogt, O. Appel, F. Riehle, and U. Sterr, Phys. Rev. Lett. **103**, 130401 (2009).
[17] S. Stellmer, M. K. Tey, B. Huang, R. Grimm, and F. Schreck, Phys. Rev. Lett. **103**, 200401 (2009).
[18] Y. N. Martinez de Escobar, P. G. Mickelson, M. Yan, B. J. DeSalvo, S. B. Nagel, and T. C. Killian, Phys. Rev. Lett. **103**, 200402 (2009).
[19] T. Fukuhara, S. Sugawa, M. Sugimoto, S. Taie, and Y. Takahashi, Phys. Rev. A **79**, 041604 (2009).
[20] P. G. Mickelson, Y. N. Martinez de Escobar, M. Yan, B. J. DeSalvo, and T. C. Killian, Phys. Rev. A **81**, 051601(R) (2010).
[21] B. J. DeSalvo, M. Yan, P. G. Mickelson, Y. N. Martinez de Escobar, and T. C. Killian, Phys. Rev. Lett. **105**, 030402 (2010).
[22] M. K. Tey, S. Stellmer, R. Grimm, and F. Schreck, Phys. Rev. A **82**, 011608 (2010).
[23] S. Taie, Y. Takasu, S. Sugawa, R. Yamazaki, T. Tsujimoto, R. Murakami, and Y. Takahashi, Phys. Rev. Lett. **105**, 190401 (2010).
[24] S. Stellmer, B. Pasquiou, R. Grimm, and F. Schreck, Phys. Rev. Lett. **110**, 263003 (2013).
[25] K. R. A. Hazzard, V. Gurarie, M. Hermele, and A. M. Rey, Phys. Rev. A **85**, 041604(R) (2012).
[26] Z. Cai, H.-H. Hung, L. Wang, D. Zheng, and C. Wu, Phys. Rev. Lett. **110**, 220401 (2013).
[27] R. Assaraf, P. Azaria, M. Caffarel, and P. Lecheminant, Phys. Rev. B **60**, 2299 (1999).
[28] M. Hermele, V. Gurarie, and A. M. Rey, Phys. Rev. Lett. **103**, 135301 (2009).
[29] T. A. Tòth, A. M. Läuchli, F. Mila, and K. Penc, Phys. Rev. Lett. **105**, 265301 (2010).
[30] S. R. Manmana, K. R. A. Hazzard, G. Chen, A. E. Feiguin, and A. M. Rey, Phys. Rev. A **84**, 043601 (2011).
[31] P. Corboz, A. M. Läuchli, K. Penc, M. Troyer, and F. Mila, Phys. Rev. Lett. **107**, 215301 (2011).
[32] A. Rapp and A. Rosch, Phys. Rev. A **83**, 053605 (2011).
[33] H. Nonne, E. Boulat, S. Capponi, and P. Lecheminant, Mod. Phys. Lett. B **25**, 955 (2011).
[34] M. Hermele and V. Gurarie, Phys. Rev. B **84**, 174441 (2011).
[35] L. Bonnes, K. R. A. Hazzard, S. R. Manmana, A. M. Rey, and S. Wessel, Phys. Rev. Lett. **109**, 205305 (2012).
[36] L. Messio and F. Mila, Phys. Rev. Lett. **109**, 205306 (2012).
[37] P. Corboz, K. Penc, F. Mila, and A. M. Läuchli, Phys. Rev. B **86**, 041106 (2012).
[38] P. Corboz, M. Lajkó, A. M. Läuchli, K. Penc, and F. Mila, Phys. Rev. X **2**, 041013 (2012).
[39] B. Bauer, P. Corboz, A. M. Läuchli, L. Messio, K. Penc, M. Troyer, and F. Mila, Phys. Rev. B **85**, 125116 (2012).
[40] Z. Cai, H.-H. Hung, L. Wang, and C. Wu, Phys. Rev. B **88**, 125108 (2013).
[41] N. Blümer and E. V. Gorelik, Phys. Rev. B **87**, 085115 (2013).
[42] H. Song and M. Hermele, Phys. Rev. B **87**, 144423 (2013).
[43] D. Wang, Y. Li, Z. Cai, Z. Zhou, Y. Wang, and C. Wu, Phys. Rev. Lett. **112**, 156403 (2014).
[44] Z. Zhou, Z. Cai, C. Wu, and Y. Wang, Phys. Rev. B **90**, 235139 (2014).
[45] P. W. Anderson, Science **235**, 1196 (1987).
[46] S.-S. Lee and P. A. Lee, Phys. Rev. Lett. **95**, 036403 (2005).
[47] Y.-J. Lin, R. L. Compton, K. Jimènez-García, J. V. Porto, and I. B. Spielman, Nature (London) **462**, 628 (2009).
[48] J. Dalibard, F. Gerbier, G. Juzeliūnas, and P. Öhberg, Rev. Mod. Phys. **83**, 1523 (2011).
[49] M. Aidelsburger, M. Atala, S. Nascimbène, S. Trotzky, Y.-A. Chen, and I. Bloch, Phys. Rev. Lett. **107**, 255301 (2011).
[50] J. Struck, C. Ölschläger, M. Weinberg, P. Hauke, J. Simonet, A. Eckardt, M. Lewenstein, K. Sengstock, and P. Windpassinger, Phys. Rev. Lett. **108**, 225304 (2012).
[51] N. Goldman, G. Juzeliunas, P. Ohberg, and I. B. Spielman, Rep. Prog. Phys. **77**, 126401 (2014).
[52] M. Aidelsburger, M. Atala, M. Lohse, J. T. Barreiro, B. Paredes, and I. Bloch, Phys. Rev. Lett. **111**, 185301 (2013).
[53] H. Miyake, G. A. Siviloglou, C. J. Kennedy, W. C. Burton, and W. Ketterle, Phys. Rev. Lett. **111**, 185302 (2013).
[54] G. Jotzu, M. Messer, R. Desbuquois, M. Lebrat, T. Uehlinger, D. Greif, and T. Esslinger, Nature (London) **515**, 237 (2014).
[55] J. Ruostekoski, G. V. Dunne, and J. Javanainen, Phys. Rev. Lett. **88**, 180401 (2002).
[56] D. Jaksch and P. Zoller, New J. Phys. **5**, 56 (2003).
[57] F. Gerbier and J. Dalibard, New J. Phys. **12**, 033007 (2010).
[58] This is a nondimensionalized flux: It is divided by a unit flux quantum so Φ is identical to the phase acquired around a single plaquette.
[59] S. Florens and A. Georges, Phys. Rev. B **70**, 035114 (2004).

[60] See Supplemental Material at http://link.aps.org/supplemental/10.1103/PhysRevA.93.061601 for detailed description of variational states used to determine the phase diagram.
[61] X. G. Wen, F. Wilczek, and A. Zee, Phys. Rev. B **39**, 11413 (1989).
[62] V. Kalmeyer and R. B. Laughlin, Phys. Rev. B **39**, 11879 (1989).
[63] P. A. Lee and N. Nagaosa, Phys. Rev. B **46**, 5621 (1992).
[64] S.-S. Lee, Phys. Rev. B **78**, 085129 (2008).
[65] S.-S. Lee, Phys. Rev. B **80**, 165102 (2009).
[66] D. F. Mross, J. McGreevy, H. Liu, and T. Senthil, Phys. Rev. B **82**, 045121 (2010).
[67] D. Dalidovich and S.-S. Lee, Phys. Rev. B **88**, 245106 (2013).
[68] T. Senthil, Phys. Rev. B **78**, 045109 (2008).
[69] W. Chen, M. P. A. Fisher, and Y.-S. Wu, Phys. Rev. B **48**, 13749 (1993).
[70] X.-G. Wen and Y.-S. Wu, Phys. Rev. Lett. **70**, 1501 (1993).
[71] A. J. Daley, M. M. Boyd, J. Ye, and P. Zoller, Phys. Rev. Lett. **101**, 170504 (2008).
[72] K. R. A. Hazzard (unpublished).
[73] X.-G. Wen, Phys. Rev. B **65**, 165113 (2002).
[74] E. Tang, M. P. A. Fisher, and P. A. Lee, Phys. Rev. B **87**, 045119 (2013).
[75] D. Ixert, F. F. Assaad, and K. P. Schmidt, Phys. Rev. B **90**, 195133 (2014).
[76] M. S. Scheurer, S. Rachel, and P. P. Orth, Sci. Rep. **5**, 8386 (2015).